Connexin43 Mimetic Peptide Improves Retinal Function and Reduces Inflammation in a Light-Damaged Albino Rat Model

Cindy X. Guo,[1,2] Mohd N. Mat Nor,[1,2] Helen V. Danesh-Meyer,[2,3] Kirstan A. Vessey,[4] Erica L. Fletcher,[4] Simon J. O'Carroll,[5] Monica L. Acosta,[1,2] and Colin R. Green[2,3]

[1]School of Optometry and Vision Science, University of Auckland, Auckland, New Zealand
[2]New Zealand National Eye Centre, University of Auckland, Auckland, New Zealand
[3]Department of Ophthalmology, University of Auckland, Auckland, New Zealand
[4]Department of Anatomy and Neuroscience, University of Melbourne, Parkville, Australia
[5]Department of Anatomy and Medical Imaging, University of Auckland, Auckland, New Zealand

Correspondence: Monica L. Acosta, School of Optometry and Vision Science, University of Auckland, New Zealand; m.acosta@auckland.ac.nz.

Submitted: February 8, 2015
Accepted: June 4, 2016

Citation: Guo CX, Mat Nor MN, Danesh-Meyer HV, et al. Connexin43 mimetic peptide improves retinal function and reduces inflammation in a light-damaged albino rat model. *Invest Ophthalmol Vis Sci*. 2016;57:3961–3973. DOI:10.1167/iovs.15-16643

Purpose. Drugs that regulate connexin43 (Cx43) gap junction channels can reduce the spread of injury and improve functional outcomes after nervous system trauma. In the eye, Cx43 expression increases in the choroid following light damage. The aim of this study was to investigate whether Cx43 hemichannel block could preserve retinal function postinjury.

Methods. Light damage was induced by exposure of adult albino Sprague-Dawley rats to 2700 Lux light for 24 hours. Intravitreal injections of a Cx43 mimetic peptide hemichannel blocker, Peptide5, or sham were administered 2 hours after the onset and at the end of the light damage period. Retinal function was assessed by electroretinogram and inflammatory responses in the choroid and retina were assessed using immunohistochemistry (ionized calcium binding adaptor molecule 1 [Iba-1], leukocyte common antigen [CD45], glial fibrillary acidic protein [GFAP]).

Results. Light-damaged rat eyes had (1) reduced neuronal responses in both the rod and cone pathways and (2) marked inflammatory responses in the choroid and retina. Peptide5 significantly preserved function of photoreceptoral and postphotoreceptoral neurons in these animals. This was evident 24 hours after injury and 2 weeks later, as shown by improved mixed a-wave and mixed b-wave amplitudes, isolated rod PII and PIII amplitudes, and cone PII responses when compared with sham-treated controls. Retinal thinning and inflammation were also significantly reduced in Peptide5-treated eyes when compared with sham-treated controls.

Conclusions. Blocking Cx43 hemichannels after light damage can significantly improve functional outcomes of neurons in both the rod and cone photo-transduction pathways in the light-damaged animal model, likely by reducing choroid inflammation and suppressing the glial-mediated inflammatory response. These data may have relevance for the treatment of conditions such as diabetic retinopathy and age-related macular degeneration.

Keywords: choroid, retina, light damage, connexin43, inflammation, electroretinogram

The choroid is the primary vascular structure supplying oxygen and nutrients to the outer neural retina. Many retinopathies are associated with choroidal degradation, such as diabetic retinopathy and age-related macular degeneration (AMD).[1–3] Thinning of the choroid, decreased choroid blood vessel density, and reduced choroid blood circulation precede the pathogenesis of both early and late stages of AMD.[3–6] It is intriguing to consider the possible role of choriocapillaris degradation in drusen formation between the Bruch's membrane and the retinal pigment epithelium and chronic inflammation with activated macrophages found in the choroid from patients with AMD.[7,8] It has also been suggested that proinflammatory and angiogenic cytokines released from activated macrophages/monocytes in the choroid contribute to progression to the more severe neovascular stage of AMD.[7,9]

In the central nervous system, connexin 43 (Cx43) is the most ubiquitous gap junction protein and is primarily expressed in astrocytes and the vascular endothelium.[10,11] It is recognized as playing an important role in the inflammatory responses.[12–14] In human and rat retinae, Cx43 is mainly expressed in Müller cells, astrocytes, vascular endothelium, and retinal pigment epithelium.[15–18] Increased Cx43 immunoreactivity has been shown in human retina associated with glaucoma[19] and following optic nerve injury.[20] In a light-damaged albino rat, Cx43 expression is significantly elevated in the choroid within 6 hours following light damage.[21] It has been suggested that the opening of Cx43 hemichannels may be involved in adenosine triphosphate (ATP) depletion, which causes necrosis and/or apoptosis,[22] and also in ATP release, a key mediator of the inflammasome pathway.[23] Cx43 hemichannel opening has also been found in endothelial cells exposed to hypoxia as well as endothelial cell death and vessel leak.[24,25]

Cx43 mimetic peptides reduce inflammation by blocking connexin hemichannels.[26,27] Peptide5, the Cx43 mimetic

peptide used in this study, reduces lesion spread and inflammation and has neuroprotective effects following spinal cord injury leading to improved functional outcomes.[26,27] Local brain administration of Peptide5 via an intracerebroventricular catheter also led to significantly improved brain functional outcomes in a model of fetal sheep global cerebral ischemia induced by bilateral carotid artery occlusion[28] and asphyxia[29] as well as in a retinal ischemia-reperfusion rat model where systemic administration of Peptide5 prevented vessel leak and reduced inflammation, with a downstream neuroprotective effect on retinal ganglion cells.[24]

The present study investigated the effect of blocking Cx43 hemichannels on retinal function in the light-damaged albino rat, an acute injury model but one that shows some of the inflammation characteristics of AMD.[30] We hypothesized that applying Peptide5 would lead to downregulation of the inflammatory response in the damaged ocular tissue, reducing the extent of damage and limiting loss of retinal function. Optical coherence tomography (OCT) and fundus imaging were used to assess changes in retinal and choroid structure. The electroretinogram (ERG) was employed in the assessment of retinal function, and microglia- and macrophage-mediated inflammatory responses were investigated in the ocular tissues.

Methods

Animals

Adult Sprague-Dawley (SD) rats (200–250 grams, male or female) were used in this study. A total of 33 rats were used in the present study: 12 rats were used for validation of the light-damaged (LD) animal model (six rats in the light-damaged group and six rats in the non–light-damaged control group); 13 rats were used for the evaluation of Peptide5 short-term effect (seven rats in the Peptide5-treated group and six rats in the sham-treated group); eight rats were used for the evaluation of the Peptide5 long-term effect (four rats were used in the Peptide5-treated group and four rats in the sham-treated group). The SD rat is an albino strain which allows the induction of photoreceptor degeneration in adult animals.[30–32] Animals were sourced from the Vernon Jansen Unit at the University of Auckland (Auckland, New Zealand). Animals were born and housed in normal cyclic light conditions (12 hours light [174 lux]:12 hours dark [< 62 lux]) until exposed to the intense light protocol. All experimental procedures described in this study were approved by the University of Auckland Animal Ethics Committee and were in compliance with the guidelines for the use of animals in vision research established by the Association for Research in Vision and Ophthalmology.

Light Damage Procedure

To induce light damage, adult SD rats were exposed to bright light for 24 hours. Light exposure started consistently around 9:00 AM to minimize damage caused by variations in time-of-day exposure.[33] The light luminance was 2700 lux, created by placing fluorescent light lamps (Philips Master TLD 18W/965; Koninklijke Philips Electronics N.V., Shanghai, China) directly above the rat cages. The light source covered broad-band fluorescence from 380 to 760 nm, with no extra heat generated. The average intensity at the top of the cage was 120 W/m^2. This broad-band fluorescence light has been used in previous studies on albino rats.[21,32] The light damage process was continuous otherwise, except for approximately 10 minutes interruption in the treatment groups (both Peptide5- and sham-treated groups) because of anesthesia and the first dose treatment. Animals were able to move freely in the cage and had access to food and water at libidum. Non–light-damaged SD rats were used as control animals.

Preparation of Cx43 Mimetic Peptide

For experiments involving Cx43 hemichannel blockade, we used Peptide5, a synthetic peptide designed to match sequences in the second extracellular loop of Cx43.[34] The peptide (H-Val-Asp-Cys-Phe-Leu-Ser-Arg-Pro-Thr-Glu-Lys-Thr-OH; molecular weight: 1396) targets Cx43 extracellular loops and was custom manufactured by Auspep Pty. Ltd (Tullamarine, Australia).[26] The peptide was purified by high-performance liquid chromatography and the structure confirmed by analytical high-performance liquid chromatography and mass spectral analysis. For delivery, Peptide5 was dissolved in saline (0.9% NaCl solution), and 4 μL of 280 μM Peptide5 was injected to achieve 20 μM as the final concentration in the vitreous based on an estimated rat vitreous volume of 56 μL.[35] The final 20 μM predicted concentration was expected to prevent hemichannel opening but not to uncouple gap junctions.[26] In a preliminary experiment, fluorescein isothiocyanate–conjugated Peptide5 was employed to ensure permeability of the peptide as far as the choroid following intravitreal injection, but all subsequent experiments were with unmodified peptide. An intravitreal injection of an equivalent volume of vehicle (saline) was used as sham control.

Administration of Cx43 Mimetic Peptide

Preliminary results from animals treated with one dose of the peptide before or after light damage or two doses at various time points indicated that a treatment regime that consists of drug administrations at 2 hours following the initiation and immediately at cessation of the intense light exposure was the most effective.

During the injections, animals were deeply anesthetized with an intraperitoneal injection of ketamine (75 mg/kg) and domitor (0.5 mg/kg). After the animals were fully anesthetized, 4 μL of either Peptide5 or sham was injected into the vitreous of both eyes either during or after the light exposure protocol (because both eyes are by necessity exposed to the light damage). Warm water bottles were used to maintain body temperature during recovery from anesthesia. A Hamilton syringe (GasTight #1705, Hamilton Co., Reno, NV, USA) with maximal volume of 10 μL attached to a 30 G × ½ needle Precision Glide TM (Becton Dickinson & Co., Franklin Lakes, NJ, USA) was used for the injection. To avoid damage to the lens, the injection was made gently to the temporal side of the eye after rotating the eyeball to the nasal side by holding the bulbar conjunctiva. The lens clarity remained the same following intravitreal injections in all of the rats included in the present study. The animals were then injected with atipamezole (1 mg/kg) to reverse the sedative effects and the intense light exposure protocol continued for additional 22 hours.

ERG Recording

The procedure was adapted and modified based on a previous study.[36] Animals were dark-adapted overnight for 12 to 14 hours before being anesthetized for the ERG recordings, which were taken 24 hours and 2 weeks after the light damage period. The pupil was dilated with 1% Tropicamide (Bausch & Lomb New Zealand Ltd., Auckland, New Zealand), and the cornea was maintained hydrated with 1% carboxymethylcellulose sodium (Celluvisc, Allergan, CA, USA) throughout the entire ERG recording process. Electroretinograms were recorded simulta-

Investigative Ophthalmology & Visual Science

neously from both eyes using homemade silver chloride electrodes. The active electrode was U-shaped and kept in contact with the center of the cornea. The inactive electrode was V-shaped and was hooked around the front teeth and in contact with the wet tongue. Body temperature was maintained at 37°C with a warm water bottle. The light stimulus was generated from a photographic flash unit (Nikon SB900 flash; Nikon, Tokyo, Japan) via a Ganzfeld sphere and elicited twin-flashes with stimulus intervals of 0.8 milliseconds. Flash intensity range was from −3.9 to 2.1 log cd.s/m^2 attained using neutral density filters. Waveforms were recorded by using Scope software (AD Instruments, Bella Vista, NSW, Australia).

ERG Data Analysis

The method of ERG analysis was reported in a previous study[36] and adapted to our experimental conditions. The a-wave reflects the rod photoreceptor response with postphotoreceptor response reflected by the b-wave. The amplitude of the a-wave was measured between the prestimulus baseline and the trough of the waveform. The amplitude of b-wave was measured between the a-wave trough and the peak of the waveform or between the baseline and the peak of the waveform if there was no a-wave. The implicit times of a- and b-waves were measured from the stimulus onset to the trough of the a-wave or the peak of the b-wave, respectively.[36,37]

The amplitudes of a- and b-waves from the mixed-rod and cone responses were plotted as a function of intensity and modeled using the Michaelis-Menten function.[38] The equation used was the following:

$$R = R_{\max} \times \frac{I^n}{I^n + K^n}$$

where $R_{\max}$ (μV) is the maximum amplitude, I (log cd.s/m^2) is the stimulus intensity, n is an exponent related to the slope of the function, and K (log cd.s/m^2) is the intensity for semisaturation. At the highest intensity light response (2.1 log cd/m^2), the rod and cone pathway waveforms were isolated using a twin flash paradigm and modelled. For the rod response, the a-wave was modeled (rod PIII) using a nonlinear function.[39] The equation was the following:

$$PIII(i \times t) = \left\{1 - \exp\left[-1/2 \times i \times S \times (t - t_d)^2\right]\right\} \times R_{\max}$$

In this equation, *PIII* represents the current generated by all the photoreceptors as a function of stimulus intensity (*i,* cd.s/m^2) and time (*t,* seconds). $R_{\max}$ (μV) is the saturated amplitude from the stimulus; S (sensitivity) characterizes the gain of photo-transduction process (m^2 / cd × s^3), and t_d (seconds) is the time latency between the stimulus onset and the start of the response.

The rod b-wave was isolated by subtracting the Rod PIII from the raw waveform and modeled (Rod PII) using an inverted gamma function. The oscillatory potentials (OPs) are another way of investigating inner retinal function. OPs were isolated by subtracting the raw b-wave from the rod PII.[36,40] Both the summed amplitude and implicit time of OPs 2, 3, and 4 were analyzed.

Optical Coherence Tomography Imaging

A spectral-domain optical coherence tomography (SD-OCT; Micron IV; Phoenix Research Laboratories, Pleasanton, CA, USA) was employed to investigate the thickness of the retinal layers in Peptide5- or sham-treated LD rats. This procedure was performed immediately after ERG recordings under the same anesthesia and pupil dilation.[41] Rats were placed on a 37°C heating pad to keep body temperature and to prevent the development of cold cataracts. Dilated eyes were covered with Poly Gel (containing 3 mg/g Carbomer; Alcon Laboratories, Pty Ltd., New South Wales, Australia), and the retina was imaged by approaching the OCT lens to the gel. StreamPix 6 software, version 7.2.4.2 (Phoenix Research Laboratories) was employed for image acquisition. The SD-OCT horizontal line B-scan had 2 μm axial resolution and consisted of 1024 pixels per A-scan. Ten B-scans, acquired 2 mm from the optic nerve in the dorsal retina, were taken and averaged. Images were analyzed using InSight software, version 1.1.5207 (Phoenix Research Laboratories) to calculate the thickness of the retinal layers. Total retinal thickness was measured from the retinal pigment epithelium to the edge of the nerve fibre layer. The thickness of the inner and outer nuclear layers were also measured.

Tissue Collection and Processing

After completion of the ERG recordings and OCT scanning (where it applies), rats were perfused transcardially with saline for 2 to 3 minutes followed by 4% paraformaldehyde in a 0.1 M phosphate buffer under anesthesia. The detailed protocol has been described in a previous study.[21] The tissue was fixed in 4% paraformaldehyde for 30 minutes, followed by washing in 0.1 M phosphate buffer saline (PBS) pH 7.4. The tissue was then cryo-protected in 10%, then 20% sucrose solutions at room temperature for 30 minutes each and in 30% sucrose solution at 4°C overnight. The tissue was then embedded and mounted in optimum cutting temperature compound (Sakura Finetek, Torrance, CA, USA) and cryo-sectioned (16-μm section thickness) in the vertical plane to the retina using a Leica CM3050 S cryostat (Leica, Heidelberg, Germany). The sections were collected onto Superfrost Plus slides (Labserv, Auckland, New Zealand), and the slides were stored at −20°C until required for immunolabeling or staining procedures.

Immunohistochemistry and Imaging

Frozen tissue sections were thawed at room temperature for 10 minutes and washed in 0.1 M PBS. Excess moisture was removed and sections were encircled with a PAP pen (Life Technologies, Camarillo, CA, USA). Sections were blocked with 6% normal goat serum (Sigma-Aldrich Corp., St. Louis, MO, USA) or normal donkey serum (Invitrogen, Frederick, MD, USA), 1% bovine serum albumin, and 0.5% Triton X-100 in 0.1 M PBS for 1 hour at room temperature. The primary antibodies (Table 1) were diluted in 0.1 M PBS containing 3% normal goat serum or normal donkey serum, 1% bovine serum albumin, and 0.5% Triton X-100 and were applied overnight in a volume sufficient to cover the tissue sections. Slides were then washed in 0.1 M PBS three times for 5 minutes each and once for 15 minutes. Secondary antibodies, goat anti-rabbit or goat anti-mouse conjugated to either Alexa 488 or Alexa 594 (Life Technologies, Carlsbad, CA, USA) were diluted 1:500 in antibody solution and applied to the sections for 2 hours at room temperature. Slides were then washed thoroughly with 0.1 M PBS, incubated with 4′,6-diamidino-2-phenylindole (Sigma-Aldrich Corp.) 1 μg/mL in 0.1 M PBS for 15 minutes to label cell nuclei, and washed again. Negative controls were processed following an identical protocol except for incubating with primary antibody solution only or secondary antibodies only. Sections were then mounted in an antifading medium (Citifluor, London, UK), and coverslips were sealed with nail polish.

All images for immunohistochemically labeled sections were acquired from the superior-central retina. Images were acquired using a confocal laser scanning microscope (Olympus FluoView FV1000; Olympus Corporation, Tokyo, Japan) with 405, 473, and/or 559 nm wavelength excitation. A series of

Table 1. List of Primary Antibodies Used in This Study

Antibody	Production	Host	Working Dilution	Company	Cat No.	Immunogen	Reference
Anti-CD45	Monoclonal, clone OX-1	Ms	1:20	BD Pharmingen, USA	550566	CD45-enriched glycoprotein fraction from Wistar rat thymocytes	21, 69
Anti-GFAP	Monoclonal, clone G-A-5 Cy3 conjugate	Ms	1:1000	Sigma-Aldrich, USA	C9205	The carboxy terminal Cys II fragment of GFAP and the N-terminal part of the tail sequence of the molecule	24
Anti-Iba1	Polyclonal	Gt	1:250	Abcam, USA	Ab5076	Synthetic peptide corresponding to amino acids 135-147 of human Iba1	21, 70

four to eight optical slices at 1-μm intervals were collected through each specimen, and image analysis was performed on an average intensity projection image. All images were acquired using the same settings. Six retinae obtained from different animals were analyzed for each group.

Statistical Analysis

Graphing and statistical analyses were performed using GraphPad Prism 5 (GraphPad Software, San Diego, CA, USA). All data are presented as the mean ± standard error of the mean (SEM). A 2-way analysis of variance (ANOVA) followed by a Bonferroni posttest was used in the ERG response analysis to compare the effects of stimulus intensity and light damage (control versus 24 hours post-LD). A 1-way ANOVA followed by Tukey's test was used in the OCT data analysis and in the ERG response at the intensity of 2.1 log cd.s/m^2 to compare control and LD animals. An unpaired *t*-test was used for analysis of the CD45 and ionized calcium-binding adaptor molecule-1 (Iba-1) immunolabeled cell counts to compare control and LD animals and to compare sham and Peptide5-treated groups.

Results

Light Damage Caused a Decrease in Retinal Function and Increased Inflammatory Responses in Both Choroid and Retina

The 24 hours of intense light exposure decreased retinal function measured with ERG at 24 hours after the cessation of light exposure. Representative rod and cone-mixed waveforms for control and LD rats are presented in Figure 1A. A comparison of the 24 hours post-LD group to the control group showed a general loss of mixed a- and b-wave amplitudes at all intensities (Figs. 1B–C). In particular, the a-wave reduction was significant at the last five intensities, from 0.1 to 2.1 log cd.s/m^2 ($n = 6$/group; 2-way ANOVA, $P < 0.001$; Fig. 1B) and the b-wave amplitude was significantly reduced at all but the highest flash intensity (2-way ANOVA, $P < 0.01$; Fig. 1C). Further rod and cone responses were analyzed at the stimulus intensity of 2.1 log cd.s/m^2 to determine whether the rod or cone pathways contributed to the decreased a- and b-waveforms (Figs. 1D–G). There was a significant reduction in the rod PIII amplitude and sensitivity in the 24 hours post-LD group when compared with the control rats (unpaired *t*-test, $P < 0.001$; Figs. 1D–E). A reduction was also observed in both rod and cone PII amplitude in the 24 hours post-LD group when compared with the control group (unpaired *t*-test, $P < 0.01$; Figs. 1F–G).

To investigate inflammatory responses involved in the choroid and retina following light damage, two biomarkers were used to label inflammatory cells in the ocular tissue: CD45 and Iba-1. CD45, also called the common leukocyte antigen, is expressed on all hematopoietic cells. CD45 was employed to identify inflammatory cells derived from the blood in the choroid. In control rats, a few CD45 immunolabeled cells were detected, which were limited to the inner capillary layer of the choroid (Fig. 2A). Following light damage, these cells had an enlarged, rounded morphology and were spread throughout the choroid (Fig. 2B). The number of CD45 immunopositive cells was significantly elevated in the light-damaged group when compared with the control group ($n = 6$/group; unpaired *t*-test, $P < 0.01$; Fig. 2C).

Iba-1 is a marker for microglia in the retina.[42,43] To determine the proportion of microglia activated in the retina, the cells immunolabeled with Iba-1 were counted in the inner (ganglion cell layer and inner plexiform layer), middle (inner nuclear layer and outer plexiform layer), and outer (outer nuclear layer and IS/OS area) parts of the retina. In the control rats, non-LD retina, Iba-1 expression was limited to the ganglion cell and plexiform layers. There were hardly any cells detected in the nuclear layers (Fig. 2D). Following light damage, microglia had thickened projecting processes and enlarged cell bodies (Fig. 2E, arrow). The number of microglia did not change significantly in the middle layers of the retina after light damage compared with the control rats (Fig. 2G). However, the number of microglia significantly decreased in the inner retina (unpaired *t*-test, $P < 0.01$; Fig. 2F) and significantly increased in the outer retina post-LD (unpaired *t*-test, $P < 0.01$; Fig. 2H).

Cx43 Mimetic Peptide Preserved Retinal Function in the LD Rats

Cx43 mimetic peptide, Peptide5 was delivered through intravitreal injections to block the opening of Cx43 hemichannels. A preliminary experiment showed that fluorescein isothiocyanate–conjugated Peptide5 penetrated throughout the full thickness of the retina and the choroid within 30 minutes after intravitreal injection. In subsequent experiments, unmodified Peptide5 was injected at 2 hours following the onset of LD (as injury will have started by then[32]), with a second injection delivered immediately post-LD. The mixed a-wave amplitude in Peptide5-treated rats was similar to sham-treated LD animals at the low stimulus intensities (–3.9 to –1.9 log cd.s/m^2), but a significant increase was detected in the Peptide5-treated group when compared with the sham-treated group at all intensities

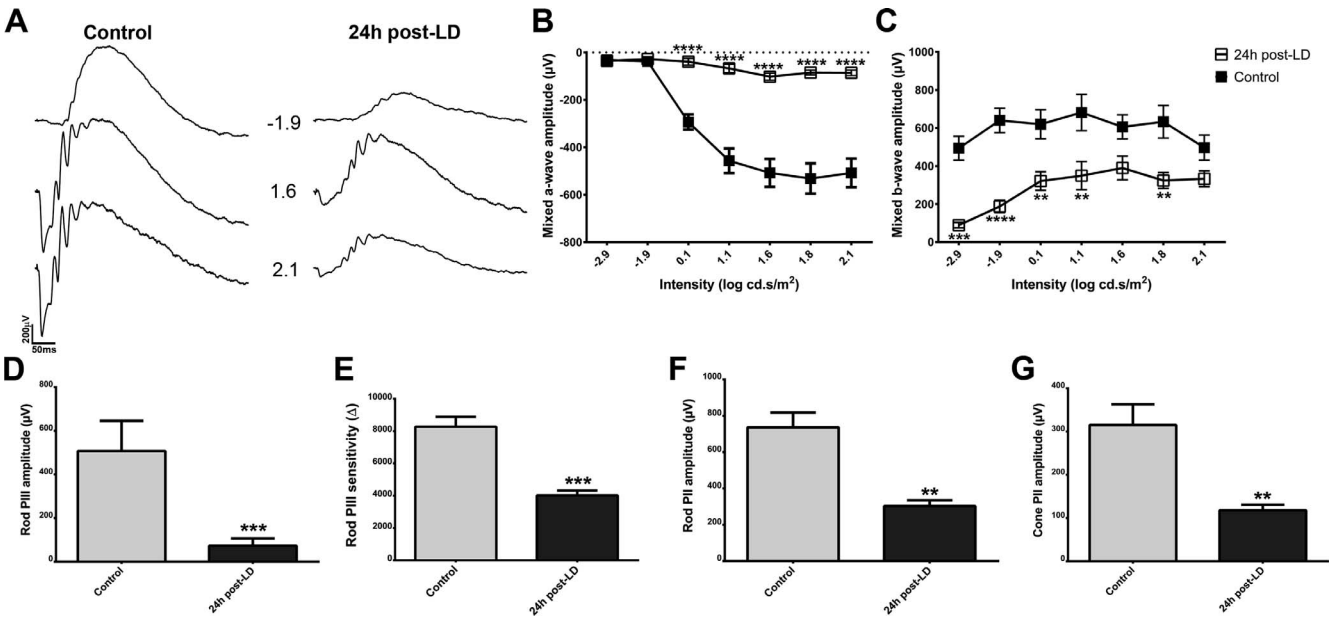

Figure 1. Reduced retinal function in LD albino rats. (**A**) Representative mixed ERG waveforms at stimulus intensities from −2.9 to 2.1 log cd.s/m^2 for non-LD control (*left*) and 24 hours post-LD rats (*right*). (**B**) The average mixed a-wave amplitude show significant reduction at intensities of 0.1 to 2.1 log cd.s/m^2 in the LD group compared with the control group (2-way ANOVA, $P < 0.001$). (**C**) The average mixed b-wave amplitude show significant reduction at intensities of −2.9 to 1.1 and 1.8 log cd.s/m^2 in the LD group compared with the control group (2-way ANOVA, $P < 0.01$). (**D–G**) Extracted average rod PIII amplitude (**D**), rod PIII sensitivity (**E**), rod PII amplitude (**F**), and cone PII amplitude (**G**) at intensity of 2.1 log cd.s/m^2 show a significant reduction in the LD group compared with the control group (unpaired *t*-test, $P < 0.01$). Data are expressed as means ± SEM ($n = 6$ in each group). Significant values are indicated with asterisks: $^{**}P < 0.01$; $^{***}P < 0.001$.

above 0.1 log cd.s/m^2 ($n = 6$/group; 2-way ANOVA, $P < 0.05$; Fig. 3A). Peptide5- and sham-treated groups showed similar implicit time for mixed a-waves (data not shown). In addition, Peptide5-treated rats had a significantly higher amplitude of mixed b-wave than that of sham-treated rats at all intensities greater than 0.1 log cd.s/m^2 (2-way ANOVA, $P < 0.01$) except for the highest flash intensity (2.1 log cd.s/m^2), which did not reach statistical significance (Fig. 3B).

The isolated rod and cone functions were also analyzed following treatment with sham or Peptide5. The rod PIII response showed significantly increased amplitude in the Peptide5-treated group (unpaired *t*-test, $P < 0.01$; Fig. 3C) and a trend toward increased sensitivity in the Peptide5-treated group when compared with the sham-treated group (Fig. 3D). Peptide5-treated animals also showed significantly increased rod PII amplitude (unpaired *t*-test, $P < 0.01$; Fig. 3E) and a similar rod PII implicit time (data not shown). The isolated cone PII response had a significantly higher amplitude (unpaired *t*-test, $P < 0.05$; Fig. 3F) and similar implicit time in Peptide5-treated group when compared with the sham-treated group (Fig. 3G). The summed OPs were not statistically significant between the Peptide5- and sham-treated groups (data not shown).

Cx43 Mimetic Peptide Reduced the Number of Inflammatory Cells in the Choroid and the Retina

Following assessment of retinal function, the inflammatory response was investigated by examining the CD45 and Iba-1 immunoreactive cells. In the choroid, there were fewer CD45-labeled cells in the Peptide5-treated group when compared with the sham-treated group (Figs. 4A, 4B). In the Peptide5-treated tissue, furthermore, the CD45$^+$ cells were in their resting state with small and oval-shaped cell bodies (arrow in Fig. 4B). Statistical analysis showed the number of CD45$^+$ cells was significantly less in the Peptide5-treated animals when compared with the sham-treated animals (unpaired *t*-test, $P < 0.001$; Fig. 4G).

Iba-1 was employed to evaluate the retinal microglial response. In sham-treated retina, Iba-1 immunolabeled microglia were located in the inner and outer nuclear layers, indicating their association with retinal neuronal cellular injury (Fig. 4C). In Peptide5-treated retina, microglia were limited to the plexiform layers and the ganglion cell layer (Fig. 4D), which is comparable to non-LD control retina (Fig. 2D). Quantification analysis showed a significant decrease in the number of microglia in the inner retinal layers (the ganglion cell layer and the inner plexiform layer, Fig. 4H) and in the middle layers (the inner nuclear layer and the outer plexiform layer, Fig. 4I) in Peptide5-treated animals when compared with sham-treated animals (unpaired *t*-test, $P < 0.05$). The Iba-1-labeled cell count in the outer retina (the outer nuclear layer and the outer segment/inner segment) showed the greatest decrease (unpaired *t*-test, $P < 0.001$; Fig. 4J).

Glial fibrillary acidic protein (GFAP) was used to examine the effect of Peptide5 on astrocyte and Müller cell activity in the retina. There was weaker immunoreactivity for GFAP in the Peptide5-treated rats when compared with the sham-treated rats (Figs. 4E–F). Stronger GFAP immunoreactivity associated with Müller cell processes was observed in sham-treated LD retina (Fig. 4E). In Peptide5-treated retina, the level of GFAP immunoreactivity remained normal and was only associated with astrocytes in the retinal nerve fibre layer (Fig. 4F).

Cx43 Mimetic Peptide Preserves Retinal Function and Protects Photoreceptors From Degeneration 2 Weeks Post–Light Damage

The long-term effect of Peptide5 was investigated after 2 weeks of recovery following the light damage. Peptide5-treated rats showed significantly improved retinal function when compared with the sham group (Fig. 5). The mixed a-wave and mixed b-

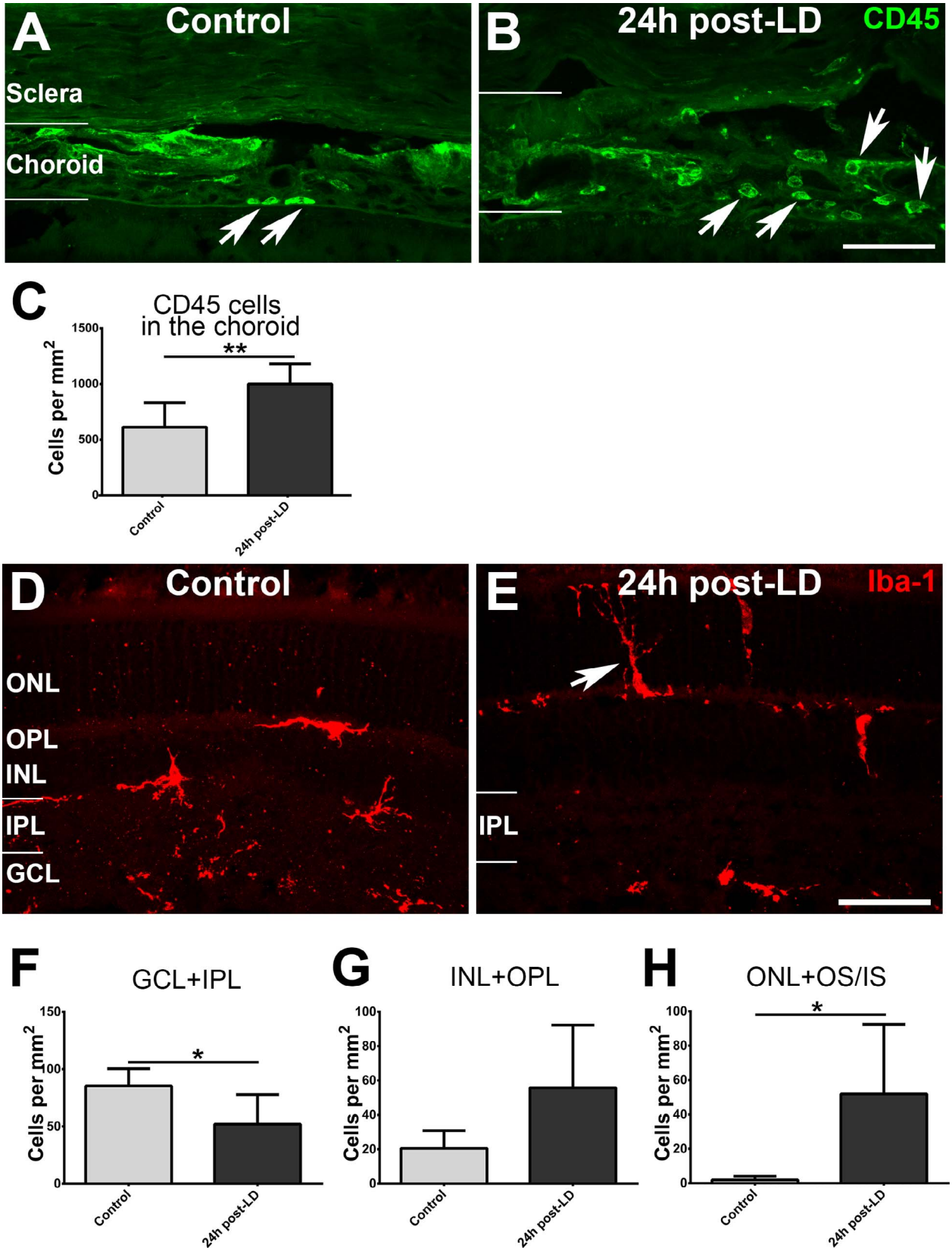

FIGURE 2. Increased inflammatory response in the choroid and the retina following light damage. (**A**, **B**) Confocal images showing CD45 immunolabeled cells in the choroid from non-LD control rat (**A**) and 24 hours post-LD (**B**). (**C**) $CD45^+$ cell count is significantly increased in the LD group compared with the control group (unpaired *t*-test, $P < 0.01$). (**D**, **E**) Confocal images showing Iba-1 immunolabeled cells in the retina from non-LD control rat (**D**) and 24 hours post-LD (**E**). (**F**–**H**) Iba-1 immunolabeled cell counts in the LD group compared with the control group in the inner retina (**F**), middle layers of the retina (**G**), and outer retina (**H**). GCL, ganglion cell layer; IPL, inner plexiform layer; INL, inner nuclear layer; OPL, outer plexiform layer; ONL, outer nuclear layer; OS/IS, outer segment/inner segment. *Scale bar*: 50 μm. Data are expressed as means ± SEM ($n = 6$ in each group). Significant values are indicated with asterisks: $^*P < 0.05$; $^{**}P < 0.01$; $^{***}P < 0.001$.

Investigative Ophthalmology & Visual Science

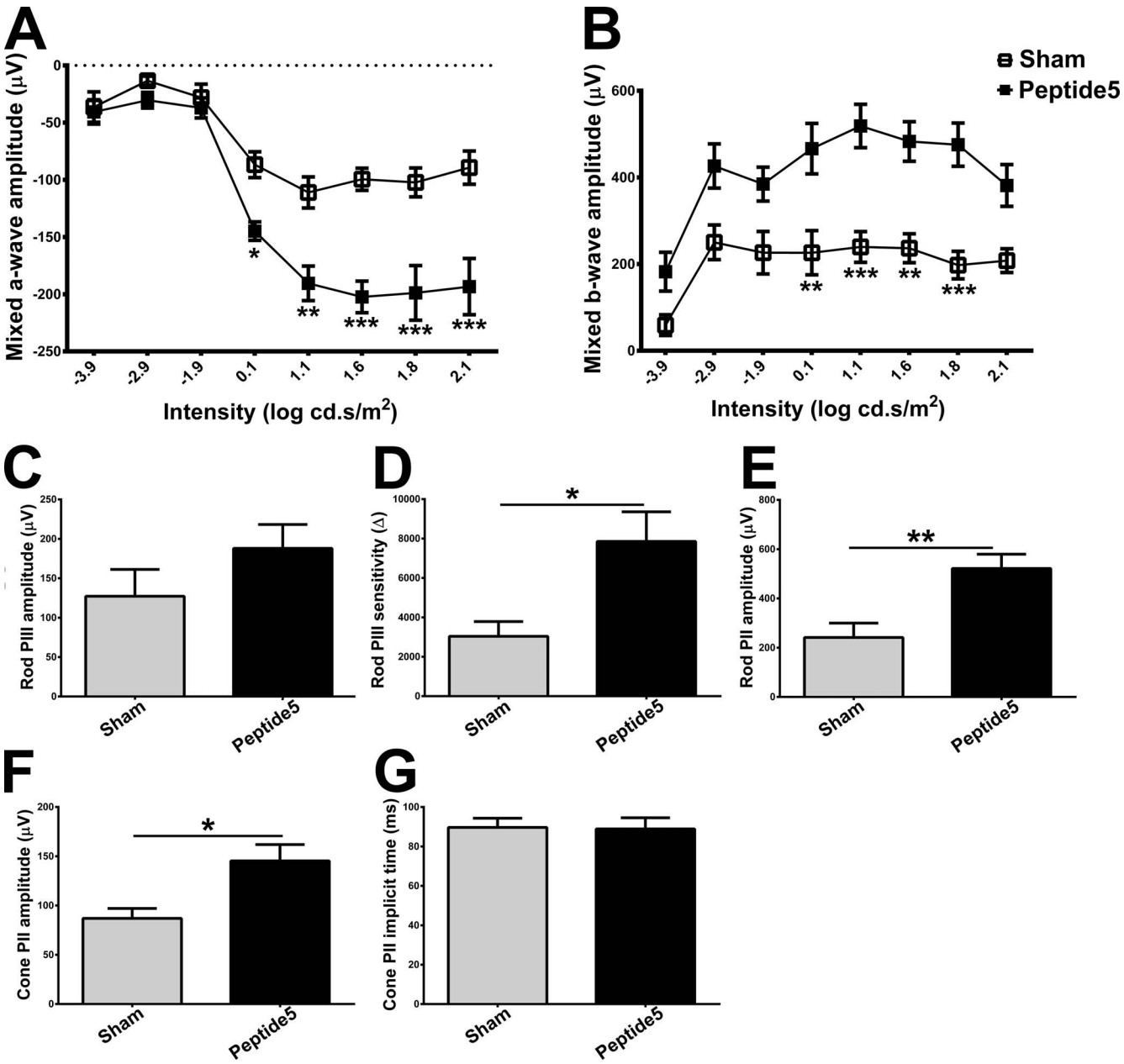

FIGURE 3. Electroretinogram analysis of LD-animals treated with Peptide5 or sham at 24 hours post-LD. (**A**) The Peptide5-treated group shows significantly improved mixed a-wave amplitude compared with the sham-treated group at stimulus intensities of 0.1 to 2.1 log cd.s/m^2 (2-way ANOVA, $P < 0.05$). (**B**) The Peptide5-treated group shows significantly improved mixed b-wave amplitude compared with the sham-treated group at stimulus intensities of 0.1 to 1.8 log cd.s/m^2 (2-way ANOVA, $P < 0.01$). (**C**–**G**) Compared with sham-treated group, Peptide5-treated groups shows improved rod and cone pathway responses at stimulus intensity of 2.1 log cd.s/m^2. There was significantly improved rod PIII amplitude (unpaired *t*-test, $P < 0.01$) (**C**), a similar rod PIII sensitivity (**D**), significantly improved rod PII amplitude (unpaired *t*-test, $P < 0.01$) (**E**), and significantly improved cone PII amplitude (unpaired *t*-test, $P < 0.05$) (**F**). There is a similar cone PII implicit time (**G**). All data are expressed as means ± SEM ($n = 7$ in Peptide5-treated group and $n = 6$ in sham-treated group). Significant values are indicated with asterisks: $^*P < 0.05$; $^{**}P < 0.01$; $^{***}P < 0.001$.

wave amplitudes at higher intensities (0.1-2.1 log cd.s/m^2) were significantly increased in the Peptide5-treated group when compared with the sham-treated group ($n = 4$/group; 2-way ANOVA, $P < 0.05$; Figs. 5A, 5B). This pattern of improvement was consistent with the mixed waveforms acquired from Peptide5- and sham-treated rats at 24 hours post-LD (Fig. 3), regardless of some photoreceptoral function recovery indicated in mixed a-wave amplitude at 2 weeks post-LD compared to 24 hours post-LD in both groups. An analysis of the isolated rod function showed significant improvement in PIII (unpaired *t*-test, $P < 0.01$; Fig. 5C) and PII amplitudes (unpaired *t*-test, $P < 0.05$; Fig. 5E) in the Peptide5-treated group when compared with the sham-treated group. Rats treated with Peptide5 also demonstrated significant improvement in cone PII amplitude when compared with the sham-treated animals (unpaired *t*-test, $P < 0.01$; Fig. 5F).

Structural changes in the retina were also investigated in Peptide5- and sham-treated rats at 2 weeks post-LD using an in vivo SD-OCT (Figs. 6A, 6B). Importantly, retinal neurons were protected from degeneration in Peptide5-treated rats, which retained significantly greater thickness of the inner (unpaired *t*-test, $P < 0.01$; Fig. 6C) and outer nuclear layers (unpaired *t*-test, $P < 0.01$; Fig. 6D) when compared with the sham-treated rats.

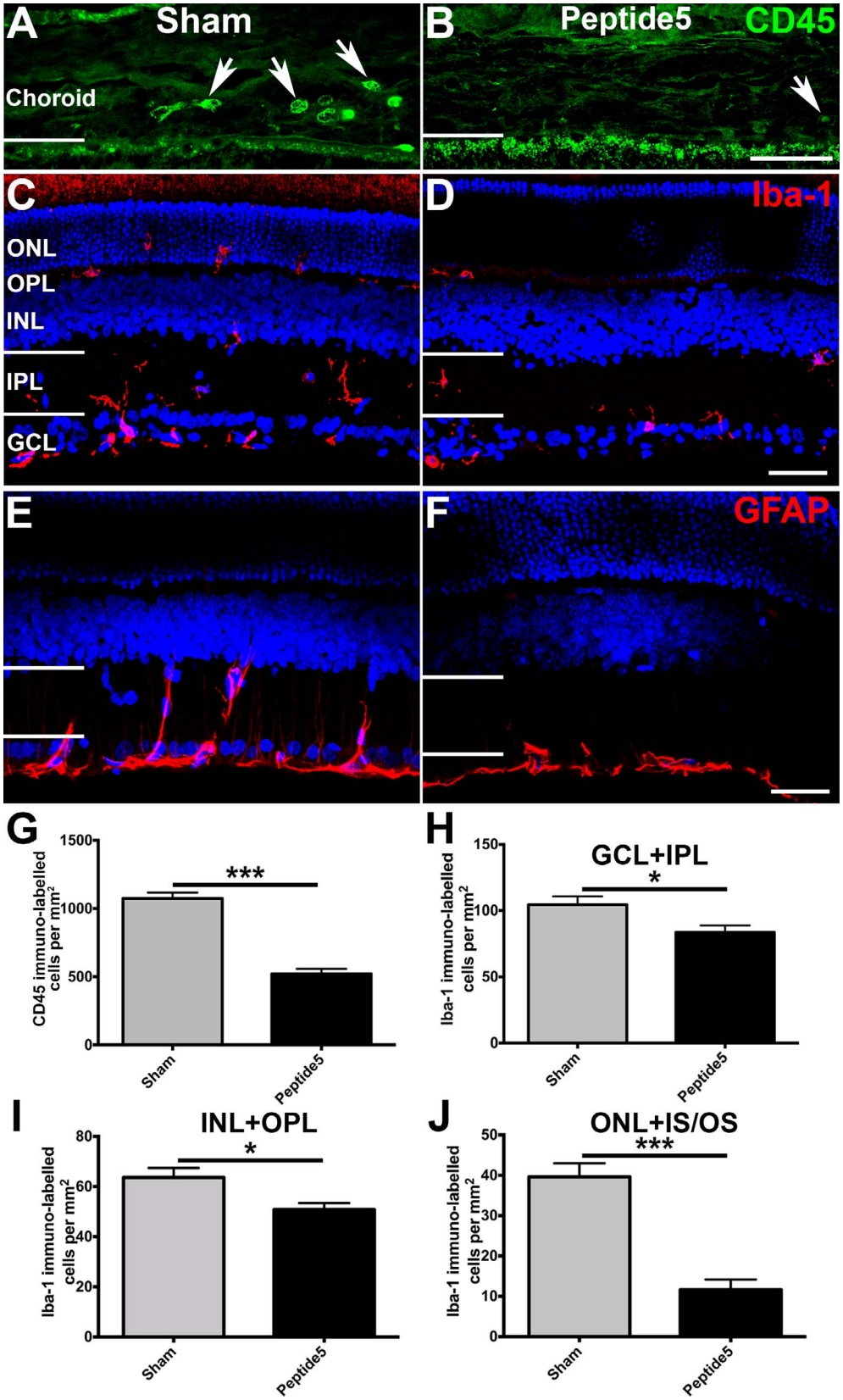

Figure 4. Administration of Peptide5 reduced inflammatory responses in the choroid and the retina in LD rats. (**A**, **B**) Confocal images show sham-treated LD rat eyes had multiple activated CD45 immunolabeled macrophages with enlarged cell bodies in the choroid (**A**, *arrows*), whereas few were seen in LD but Peptide5-treated rat eyes (**B**, *arrow*). (**C**, **D**) Confocal images show that in sham-treated rat retinae Iba-1 immunolabeled cells were detected migrating into the nuclear layers (**C**), but these cells remained mostly in the plexiform layers in Peptide5-treated rat retinae (**D**). (**E**, **F**) Elevated GFAP immunoreactivity was seen in LD- but sham-treated rat retinae (**E**) and normal GFAP immunoreactivity was detected in Peptide5-treated rat eyes (**F**). (**G**) Statistical analysis using unpaired *t*-test showed $CD45^{+}$ cell counts were significantly lower in the choroid in of the Peptide5-

Investigative Ophthalmology & Visual Science

treated group compared with the LD- but sham-treated group ($P < 0.001$). (**H–J**) Quantification analysis showed a significantly decreased number of Iba-1 immunolabeled microglia in all the layers in the LD- but Peptide5-treated group compared with the sham-treated group ($P < 0.05$). The cell count in the outer retina showed the most significant decrease (**G**; $P < 0.001$). GCL, ganglion cell layer; IPL, inner plexiform layer; INL, inner nuclear layer; OPL, outer plexiform layer; ONL, outer nuclear layer. *Scale bar*: 50 μm. All data are expressed as means ± SEM ($n = 6$ in each group). Significant values are indicated with asterisks: $^{*}P < 0.05$; $^{**}P < 0.01$; $^{***}P < 0.001$.

Discussion

Although it is an acute injury model, light damage to the eye of albino rats results in oxidative stress and inflammation in both the choroid and the retina that resemble the early pathologic events seen in AMD.[21,44] In this model, Cx43 is increased in the choroid following light damage[21] and the present study demonstrated that a Cx43 mimetic peptide, Peptide5, at a concentration considered to block hemichannels but not to uncouple gap junctions, was able to reduce the inflammatory response and preserve retinal function. Treatments with Peptide5 resulted in a better survival rate and functional response in the rod and cone pathways both short- and long-term, demonstrated by the significantly improved outcomes assessed using ERG and SD-OCT.

Intense light exposure causes extensive retinal damage, prominently on rod photoreceptors in the superior hemisphere when the lighting source is from the ceiling.[45] Retinal light damage and photoreceptor death are detectable as early as 2 hours after the initiation of intense light exposure.[32,46] Photoreceptor loss and extensive retinal remodeling remain for 60 days or more.[30,45,47] The present study demonstrated positive effects on the preservation of retinal functions and protection from retinal remodeling, with the benefits persisting in Peptide5-treated rats when compared with sham-treated animals.

In the light-damaged albino rat model, the retinal pigment epithelium (RPE) and choroid respond quickly to intense light exposure, with oxidative stress and inflammatory response peaking in the RPE/choroid before they do in the retina.[21] This damage in the RPE/choroid is thought to initiate or accelerate neuronal cell death processes in the retina following intense light exposure. The upregulation of Cx43 in the choroid correlates with increased infiltration of inflammatory cells.[21] The administration of Peptide5 significantly suppressed the macrophage-mediated inflammatory response in the choroid. Peptide5 was also effective in preventing activation of retinal microglia, which in the LD model may release neurotoxic factors, inducing neurons to start or continue the cell death process.[48] Abundant free radical nitric oxide and reactive

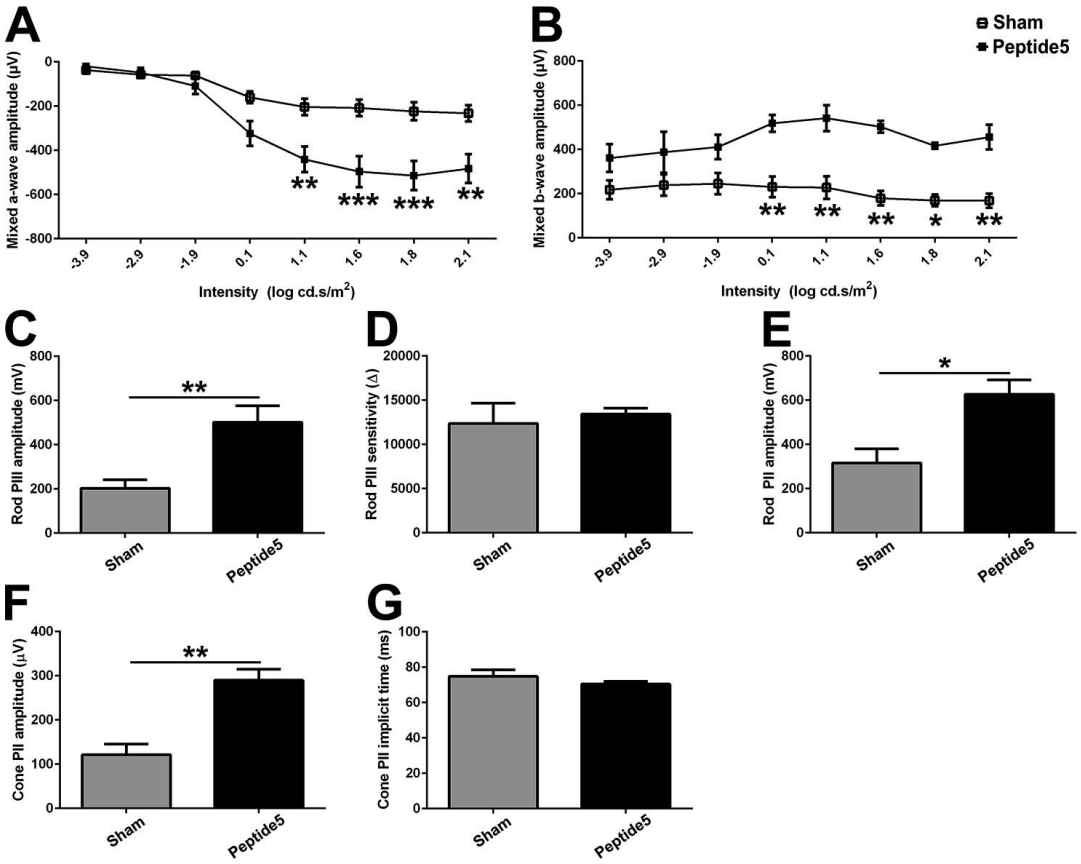

Figure 5. Electroretinogram analysis of mixed a- and b-wave responses 2 weeks after LD animals were treated with Peptide5 or sham. (**A**) The Peptide5-treated group shows significantly improved mixed a-wave amplitude compared with the sham-treated group at stimulus intensities of 0.1 to 2.1 log cd.s/m^2 (2-way ANOVA, $P < 0.05$). (**B**) The Peptide5-treated group shows significantly improved mixed b-wave amplitude compared with the sham-treated group at stimulus intensities of 0.1 to 1.8 log cd.s/m^2 (2-way ANOVA, $P < 0.01$). (**C–G**) Extracted average rod PIII amplitude (**C**), rod PIII sensitivity (**D**), rod PII amplitude (**E**), cone PII amplitude (**F**), and cone PII implicit time (**G**) at intensity of 2.1 log cd.s/m^2 show a significant reduction in amplitude in the LD-treated group compared with the sham group. Data are expressed as means ± SEM ($n = 4$ in each group). Significant values are indicated with asterisks: $^{*}P < 0.05$; $^{**}P < 0.01$; $^{***}P < 0.001$.

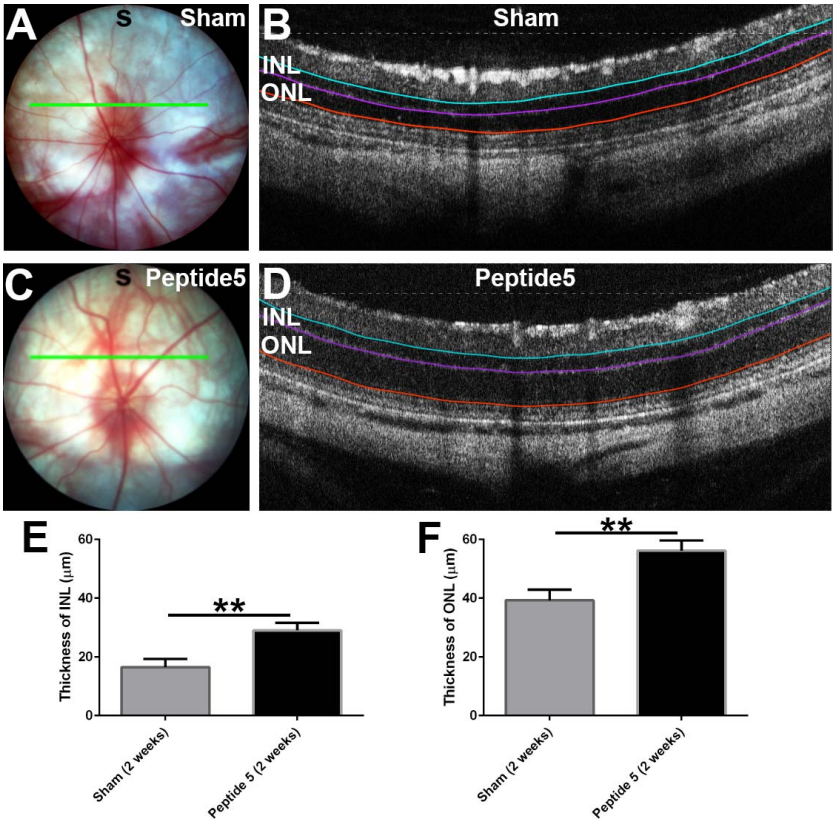

FIGURE 6. Retinal morphology treated with Peptide5 or sham at 2 weeks post-LD. Retinal morphology in sham-treated rats shown in representative fundus image (**A**) and SD-OCT image (**B**) in comparison with retinal morphology in Peptide5-treated animals shown in fundus image (**C**) and SD-OCT image (**D**). Quantification of the inner retinal layer (**E**) and the outer retinal layer (**F**) layer thickness. INL, inner nuclear layer; ONL, outer nuclear layer. All data are expressed as means ± SEM ($n = 4$ in each group). Significant values are indicated with asterisks: $^{**}P < 0.01$.

nitrogen oxides have been detected in activated microglia and have been suggested to be neurotoxic agents involved in neurodegenerative diseases.[49,50] In this study, therefore, Peptide5 appears to have abrogated a significant portion of the continuing damage spread resulting from bright light damage, with downstream benefits evident at least through to 2 weeks postinjury. Nonetheless, Marc et al.[30] have demonstrated that photoreceptor degeneration and extensive retinal remodeling may be continuing even 60 days following intense light exposure. They reported that the onset of remodeling is rapid, with immediate signs of metabolic stress in multiple cell types, including photoreceptors, the retinal pigmented epithelium, Müller cells, and the choriocapillaris. After the initial stress phase, damage progresses to focal photoreceptor degeneration within 14 days and extensive remodeling by 60 days. It will be interesting to pursue longer term studies to determine whether the benefits of Peptide5, acting during the initial damage phase, extend to this full period.

The bystander effect has been suggested to play a role in the pathogenesis of retinitis pigmentosa with apoptotic signals from dying rods transferred through intercellular gap-junctional channels to neighboring healthy cones.[51] Despite the demonstrated upregulation of connexins, we do not propose, however, that a bystander effect is evident in the effects demonstrated here. Intense light exposure causes alterations to endothelial cells of the choriocapillaris, which triggers the inflammatory response associated with Cx43 hemichannel opening. Previous in vitro and in vivo studies have suggested that Peptide5 functions by blocking the uncontrolled opening of Cx43 hemichannels,[24,26,28] which are primarily kept closed under physiological conditions.[52] Peptide5 was designed to match a portion of Cx43 extracellular loop two.[26] Under pathologic conditions, hemichannel opening causes cytoplasmic oedema (and cell rupture), and particularly Cx43 hemichannels have been identified on cytoplasmic processes of the glial cells[52–54] involved in ATP release, the onset of calcium waves[25] and activation of the inflammasome pathway,[23] and may result in the release of ATP and glutamate as well as the establishment of calcium waves.[54] Peptide5 has previously been shown to reduce vessel leak and inflammation following central nervous system (CNS) injury, promote glial and neuronal survival, or provide improved functional outcomes in several CNS models.[24,25,28,29,55] (For a full review of hemichannel roles in CNS injury, see, e.g., Refs. 23, 25, 54, 56–59.)

Peptide5 may, in addition, work directly on RPE cells because ATP-mediated paracrine intercellular communication through Cx43 hemichannels also occurs in the RPE.[60] RPE cells under oxidative stress are known to increase the release of basic fibroblast growth factor, which could lead to sustained pathologic angiogenesis in the choroid,[61] and to secrete proinflammatory factors associated with the inflammasome pathways, including Interleukin-1β, Interleukin-6, tumor necrosis factor-α, and granulocyte macrophage-colony stimulating factor.[23,62]

In particular, however, capillary dysfunction is reported to precede a number of degenerative CNS diseases, including Alzheimer's and Parkinson's disease[63–65] as well as AMD[3–6] and diabetic retinopathy.[2,66] The regulation of Cx43 channels has been shown to protect the vascular bed after retinal ischemia reperfusion and after spinal cord injury, with a corresponding reduction in the inflammatory response,[24,67] and it is of note

that in the longer term a reduction in choroid circulation has been reported to be responsible for delayed photoreceptor loss in the light damage model used in this study.[68] It remains to be seen whether Peptide5 is having a direct effect on choroidal endothelial cell survival as it does after injury in the retinal ischemia-reperfusion model.[24]

In summary, findings from the present study show that locally blocking Cx43 hemichannels with an intravitreal injection of the Cx43 channel blocking mimetic peptide, Peptide5, can significantly improve the function of neurons in the rod and cone photo-transduction pathways in the light-damaged animal model. The enhancement of neuronal functional outcomes may be achieved by reducing choroid vessel dysfunction and choroid inflammation and by suppressing the glia-mediated inflammatory response. In this study, the peptide was administered at 2 hours after the onset and immediately after the cessation of the light damage period, but significant benefits extend to at least 2 weeks postinjury. It remains to be seen whether additional optimization of delivery protocols could further improve outcomes. These results have significance for potential treatments of conditions such as diabetic retinopathy, diabetic macular oedema, and AMD.

Acknowledgments

Supported by the Health Research Council of New Zealand, the Auckland Medical Research Foundation, University of Auckland Faculty of Science Research and Development Fund, and PhD scholarship from Ministry of Higher Education Malaysia (MNMN).

Disclosure: **C.X. Guo**, None; **M.N. Mat Nor**, None; **H.V. Danesh-Meyer**, None; **K.A. Vessey**, None; **E.L. Fletcher**, None; **S.J. O'Carroll**, None; **M.L. Acosta**, None; **C.R. Green**, CoDa Therapeutics, Inc. (I)

References

1. Bird AC, Bressler NM, Bressler SB, et al. An international classification and grading system for age-related maculopathy and age-related macular degeneration. *Surv Ophthalmol*. 1995;39:367–374.
2. Regatieri CV, Branchini L, Carmody J, Fujimoto JG, Duker JS. Choroidal thickness in patients with diabetic retinopathy analyzed by spectral-domain optical coherence tomography. *Retina*. 2012;32:563–568.
3. Biesemeier A, Taubitz T, Julien S, Yoeruek E, Schraermeyer U. Choriocapillaris breakdown precedes retinal degeneration in AMD. *Neurobiol Aging*. 2014;35:2562–2573.
4. Metelitsina TI, Grunwald JE, DuPont JC, Ying G-S, Brucker AJ, Dunaief JL. Foveolar choroidal circulation and choroidal neovascularization in age-related macular degeneration. *Invest Ophthalmol Vis Sci*. 2008;49:358–363.
5. Chung SE, Kang SW, Lee JH, Kim YT. Choroidal thickness in polypoidal choroidal vasculopathy and exudative age-related macular degeneration. *Ophthalmology*. 2011;118:840–845.
6. Mullins RF, Johnson MN, Faidley, EA, Skeie, JM, Huang J. Choriocapillaris vascular dropout related to density of drusen in human eyes with early age-related macular degeneration. *Invest Ophthalmol Vis Sci*. 2011;52:1606–1612.
7. Penfold PL, Madigan MC, Gillies MC, Provis JM. Immunological and aetiological aspects of macular degeneration. *Prog Retin Eye Res*. 2001;20:385–414.
8. Bhutto I, Lutty G. Understanding age-related macular degeneration (AMD): relationships between the photoreceptor/retinal pigment epithelium/Bruch's membrane/choriocapillaris complex. *Mol Aspects Med*. 2012;33: 295–317.
9. Cousins SW, Espinosa-Heidmann DG, Csaky KG. Monocyte activation in patients with age-related macular degeneration: a biomarker of risk for choroidal neovascularization? *Arch Ophthalmol*. 2004;122:1013–1018.
10. Contreras JE, Sánchez HA, Véliz LP, Bukauskas FF, Bennett MVL, Sáez JC. Role of connexin-based gap junction channels and hemichannels in ischemia-induced cell death in nervous tissue. *Brain Res Rev*. 2004;47:290–303.
11. Naus CCG, Ozog MA, Bechberger JF, Nakase T. A neuroprotective role for gap junctions. *Cell Commun Adhes*. 2001;8: 325–328.
12. Bennett MVL, Garré JM, Orellana JA, Bukauskas FF, Nedergaard M, Sáez JC. Connexin and pannexin hemichannels in inflammatory responses of glia and neurons. *Brain Res*. 2012;1487: 3–15.
13. Mika T, Prochnow N. Functions of connexins and large pore channels on microglial cells: the gates to environment. *Brain Res*. 2012;1487:16–24.
14. Orellana JA, von Bernhardi R, Giaume C, Sáez JC. Glial hemichannels and their involvement in aging and neurodegenerative diseases. *Nat Rev Neurosci*. 2012;23:163–177.
15. Zahs KR, Kofuji P, Meier C, Dermietzel R. Connexin immunoreactivity in glial cells of the rat retina. *J Comp Neurol*. 2003;455:531–546.
16. Kuo IY, Chan-Ling T, Wojcikiewicz RJ, Hill CE. Limited intravascular coupling in the rodent brainstem and retina supports a role for glia in regional blood flow. *J Comp Neurol*. 2008;511:773–787.
17. Janssen-Bienhold U, Dermietzel R, Weiler R. Distribution of connexin43 immunoreactivity in the retinas of different vertebrates. *J Comp Neurol*. 1998;396:310–321.
18. Kerr NM, Johnson CS, de Souza CF, et al. Immunolocalization of gap junction protein connexin43 (GJA1) in the human retina and optic nerve. *Invest Ophthalmol Vis Sci*. 2010;51: 4028–4034.
19. Kerr NM, Johnson CS, Green CR, Danesh-Meyer HV. Gap junction protein connexin43 (GJA1) in the human glaucomatous optic nerve head and retina. *J Clin Neurosci*. 2011;18: 102–108.
20. Chew SSL, Johnson CS, Green CR, Danesh-Meyer HV. Response of retinal Connexin43 to optic nerve injury. *Invest Ophthalmol Vis Sci*. 2011;52:3620–3629.
21. Guo CX, Tran H, Green CR, Danesh-Meyer HV, Acosta ML. Gap junction proteins in the light-damaged albino rat. *Mol Vis*. 2014;20:670–682.
22. Vergara L, Bao X, Bello-Reuss E, Reuss L. Do connexin 43 gap-junctional hemichannels activate and cause cell damage during ATP depletion of renal tubule cells? *Acta Physiol Scand*. 2003;179:33–38.
23. Kim Y, Davidson JO, Gunn KC, Phillips AR, Green CR, Gunn AJ. Role of hemichannels in CNS inflammation and the inflammasome pathway. *Adv Protein Chem Struct Biol*. 2016;104:1–37.
24. Danesh-Meyer HV, Kerr NM, Zhang J, et al. Connexin43 mimetic peptide reduces vascular leak and retinal ganglion cell death following retinal ischaemia. *Brain*. 2012;135:506–520.
25. Danesh-Meyer HV, Zhang J, Acosta M, Rupenthal ID, Green CR. Connexin43 in retinal injury and disease. *Prog Retin Eye Res*. 2016;51:41–68.
26. O'Carroll SJ, Alkadhi M, Nicholson LF, Green CR. Connexin 43 mimetic peptides reduce swelling, astrogliosis, and neuronal cell death after spinal cord injury. *Cell Commun Adhes*. 2008; 15:27–42.

27. O'Carroll SJ, Gorrie CA, Velamoor S, Green CR, Nicholson LFB. Connexin43 mimetic peptide is neuroprotective and improves function following spinal cord injury. *Neurosci Res*. 2013;75: 256–267.
28. Davidson JO, Green CR, Nicholson LFB, et al. Connexin hemichannel blockade improves outcomes in a model of fetal ischemia. *Ann Neurol*. 2012;71:121–132.
29. Davidson JO, Drury PP, Green CR, Nicholson LFB, Bennet L, Gunn AJ. Connexin hemichannel blockade is neuroprotective after asphyxia in preterm fetal sheep. *PLoS One*. 2014;9: e96558.
30. Marc RE, Jones BW, Watt CB, Vazquez-Chona F, Vaughan DK, Organisciak DT. Extreme retinal remodeling triggered by light damage: implications for age related macular degeneration. *Mol Vis*. 2008;14:782–806.
31. Noell WK, Walker VS, Kang BS, Berman S. Retinal damage by light in rats. *Invest Ophthalmol*. 1966;5:450–473.
32. Yu TY, Acosta ML, Ready S, Cheong YL, Kalloniatis M. Light exposure causes functional changes in the retina: increased photoreceptor cation channel permeability, photoreceptor apoptosis, and altered retinal metabolic function. *J Neurochem*. 2007;103:714–724.
33. White MP, Fisher LJ. Degree of light damage to the retina varies with time of day of bright light exposure. *Physiol Behav*. 1987; 39:607–613.
34. Evans WH, Boitano S. Connexin mimetic peptides: specific inhibitors of gap-junctional intercellular communication. *Biochem Soc Trans*. 2001;29:606–612.
35. Berkowitz BA, Lukaszeu RA, Mullins CM, Penn JS. Impaired hyaloidal circulation function and uncoordinated ocular growth patterns in experimental retinopathy of prematurity. *Invest Ophthalmol Vis Sci*. 1998;39:391–396.
36. Vessey KA, Wilkinson-Berka JL, Fletcher EL. Characterization of retinal function and glial cell response in a mouse model of oxygen-induced retinopathy. *J Comp Neurol*. 2011;519:506–527.
37. Sun D, Bui BV, Vingrys AJ, Kalloniatis M. Alterations in photoreceptor-bipolar cell signaling following ischemia/reperfusion in the rat retina. *J Comp Neurol*. 2007;505:131–146.
38. Naka KI, Rushton WAH. S-potentials from luminosity units in retina of fish (*Cyprinidae*). *J Physiol*. 1966;185:587–599.
39. Hood DC, Birch DG. The a-wave of the human electroretinogram and rod receptor function. *Invest Ophthalmol Vis Sci*. 1990;31:2070–2081.
40. Weymouth AE, Vingrys AJ. Rodent electroretinography: methods for extraction and interpretation of rod and cone responses. *Prog Retin Eye Res*. 2008;27:1–44.
41. Liu H-H, Bui BV, Nguyen CTO, Kezic JM, Vingrys AJ, He Z. Chronic ocular hypertension induced by circumlimbal suture in rats circumlimbal suture model of glaucoma. *Invest Ophthalmol Vis Sci*. 2015;56:2811–2820.
42. Ibrahim AS, El-Remessy AB, Matragoon S, et al. Retinal microglial activation and inflammation induced by amadori-glycated albumin in a rat model of diabetes. *Diabetes*. 2011; 60:1122–1133.
43. Xu HP, Chen M, Mayer EJ, Forrester JV, Dick AD. Turnover of resident retinal microglia in the normal adult mouse. *Glia*. 2007;55:1189–1198.
44. Rutar M, Provis JM, Valter K. Brief exposure to damaging light causes focal recruitment of macrophages, and long-term destabilization of photoreceptors in the albino rat retina. *Curr Eye Res*. 2010;35:631–643.
45. Organisciak DT, Vaughan DK. Retinal light damage: mechanisms and protection. *Prog Retin Eye Res*. 2010;29:113–134.
46. Organisciak DT, Darrow RA, Barsalou L, Darrow RM, Lininger LA. Light-induced damage in the retina: differential effects of dimethylthiourea on photoreceptor survival, apoptosis and DNA oxidation. *Photochem Photobiol*. 1999;70:261–268.
47. Stone J, Maslim J, Valter-Kocsi K, et al. Mechanisms of photoreceptor death and survival in mammalian retina. *Prog Retin Eye Res*. 1999;18:689–735.
48. Marín-Teva JL, Cuadros MA, Martín-Oliva D, Navascués J. Microglia and neuronal cell death. *Neuron Glia Biol*. 2012;1: 1–16.
49. Chao C, Hu S, Molitor TW, Shaskan EG, Peterson PK. Activated microglia mediate neuronal cell injury via a nitric oxide mechanism. *J Immunol*. 1992;149:2736–2741.
50. Boje KM, Arora PK. Microglial-produced nitric oxide and reactive nitrogen oxides mediate neuronal cell death. *Brain Res*. 1992;587:250–256.
51. Ripps H. Cell death in retinitis pigmentosa: gap junctions and the "bystander" effect. *Exp Eye Res*. 2002;74:327–336.
52. Goodenough DA, Paul DL. Beyond the gap: functions of unpaired connexon channels. *Nat Rev Mol Cell Biol*. 2003;4: 285–295.
53. Hofer A, Dermietzel R. Visualization and functional blocking of gap junction hemichannels (connexons) with antibodies against external loop domains in astrocytes. *Glia*. 1998;24: 141–154.
54. Davidson JO, Green CR, Bennet L, Gunn AJ. Battle of the hemichannels–connexins and pannexins in ischemic brain injury. *Int J Dev Neurosci*. 2015;45:66–74.
55. O'Carroll SJ, Becker DL, Davidson JO, Gunn AJ, Nicholson LFB, Green CR. The use of connexin-based therapeutic approaches to target inflammatory diseases. *Wound Repair Regen*. 2013; 1037:519–546.
56. Eugenin EA, Basilio D, Sáez JC, et al. The role of gap junction channels during physiologic and pathologic conditions of the human central nervous system. *J Neuroimmune Pharmacol*. 2012;7:499–518.
57. Orellana JA, Sáez PJ, Shoji KF, et al. Modulation of brain hemichannels and gap junction channels by pro-inflammatory agents and their possible role in neurodegeneration. *Antioxid Redox Signal*. 2009;11:369–399.
58. Takeuchi H, Suzumura A. Gap junctions and hemichannels composed of connexins: potential therapeutic targets for neurodegenerative diseases. *Front Cell Neurosci*. 2014;8:1–12.
59. Decrock E, De Bock M, Wang N, et al. Connexin and pannexin signaling pathways, an architectural blueprint for CNS physiology and pathology? *Cell Mol Life Sci*. 2015;72:2823–2851.
60. Pearson RA, Dale N, Llaudet E, Mobbs P. ATP released via gap junction hemichannels from the pigment epithelium regulates neural retinal progenitor proliferation. *Neuron*. 2005;46:731–744.
61. Eichler W, Reiche A, Yafai Y, Lange J, Wiedemann P. Growth-related effects of oxidant-induced stress on cultured RPE and choroidal endothelial cells. *Exp Eye Res*. 2008;87:342–348.
62. Ma W, Zhao L, Fontainhas AM, Fariss RN, Wong WT. Microglia in the mouse retina alter the structure and function of retinal pigmented epithelial cells: a potential cellular interaction relevant to AMD. *PLoS One*. 2009;4:e7945.
63. Guan J, Pavlovic D, Dalkie N, et al. Vascular degeneration in Parkinson's disease. *Brain Pathol*. 2013;23:154–164.
64. Farkas E, Luiten PGM. Cerebral microvascular pathology in aging and Alzheimer's disease. *Prog Neurobiol*. 2001;64:575–611.

Investigative Ophthalmology & Visual Science

65. Retamal MA, Reyes EP, García IE, Pinto B, Martínez AD, González C. Diseases associated with leaky hemichannels. *Front Cell Neurosci*. 2015;9:267.
66. Tam J, Dhamdhere KP, Tiruveedhula P, et al. Disruption of the retinal parafoveal capillary network in type 2 diabetes before the onset of diabetic retinopathy. *Invest Ophthalmol Vis Sci*. 2011;52:9257–9266.
67. Cronin M, Anderson PN, Cook JE, Green CR, Becker DL. Blocking connexin43 expression reduces inflammation and improves functional recovery after spinal cord injury. *Mol Cell Neurosci*. 2008;39:152–160.
68. Tanito M, Kaidzu S, Anderson RE. Delayed loss of cone and remaining rod photoreceptor cells due to impairment of choroidal circulation after acute light exposure in rats. *Invest Ophthalmol Vis Sci*. 2007;48:1864–1872.
69. Adamis AP, Ishida S, Yamashiro K, et al. Leukocytes mediate retinal vascular remodeling during development and vaso-obliteration in disease. *Nat Med*. 2003;9:781–788.
70. Xu H, Chen M, Manivannan A, Lois N, Forrester JV. Age-dependent accumulation of lipofuscin in perivascular and subretinal microglia in experimental mice. *Aging Cell*. 2008;7:58–68.

Investigative Ophthalmology & Visual Science